Nonequilibrium Pattern Formation in Langmuir−Phase Assisted Assembly of Alkylsiloxane Monolayers

ARTICLE *in* THE JOURNAL OF PHYSICAL CHEMISTRY B · NOVEMBER 1999

Impact Factor: 3.3 · DOI: 10.1021/jp992030y

Nonequilibrium Pattern Formation in Langmuir-Phase Assisted Assembly of Alkylsiloxane Monolayers

Rong Wang,*,† Atul N. Parikh,*,† Jaime D. Beers,† Andrew P. Shreve,† and Basil Swanson†

Bioscience Division, Los Alamos National Laboratory, Los Alamos, New Mexico 87545

Received: June 18, 1999; In Final Form: August 9, 1999

Prepolymerized *n*-octadecyltrichlorosilane (OTS) monolayers were deposited onto oxidized silicon substrates from precursor Langmuir monolayers (at an air−water interface) in two-dimensional liquid expanded (LE), liquid condensed (LC), or mixed (LE/LC coexistence phase) states at four different pulling rates. Morphologies of the transferred monolayers have been investigated using atomic force microscopy (AFM). The OTS monolayers formed from the LE phase precursor reveal an incipient condensation transition exhibiting a novel ring-in-a-ring morphology, wherein uniformly distributed circular domains consisting of two concentric walls of ordered OTS molecules in a high density phase both sandwich and encapsulate disordered OTS molecules in a reduced density phase. On the other hand, the monolayers formed from the LC/LE phase precursor implicate a complete condensation transition, evidenced in the AFM images showing a uniform tiling of near-circular domains composed of ordered OTS molecules in a dense monolayer phase. The monolayers derived from the 2D solid or LC precursor state reveal near-complete surface coverages and uniform film structures, comparable to those obtained by adsorption from a dilute organic solution of OTS molecules (conventional self-assembly process). These structural reconstructions at the substrate surface, namely lateral redistribution into 2D domains, condensation transitions and film coverages, are discussed in terms of the competition between short range and long range interactions. The most dominant effect of increasing pulling rates is the appearance of coalesced domain structures, presumably due to drainage of the water layer at the substrate surface as well as occasional substrate pinning. These results substantiate the idea that templating surface self-assembly of monolayers by using their Langmuir-phase precursors provides a useful alternative to classical solution-phase self-assembly approaches, and affords a wide range of control over film structures and surface morphologies.

Introduction

Control over surface topology and defect structures has been a subject of considerable recent interest. This interest is motivated not only by the important fundamental scientific issues related to two-dimensional nucleation and growth mechanisms but also by their relevance in controlled development of spatially and topologically patterned surfaces for applications ranging from the study of biological processes to micro/nanoscale fabrication.[1−4] Within this framework, several experimental approaches have proved quite useful for organic monolayer patterning. For example, the techniques of selective self-assembly onto prepatterned substrates,[5] lithography,[6] and microcontact printing or stamping[7,8] have all been shown to allow controlled fabrication of compositional or topological patterns of predefined features and shapes at large, micrometer range scales. These approaches have been highly successful for both major classes of self-assembly chemistries, namely alkanethiols on coinage metals[9] and alkylsiloxanes on oxide substrates.[10] Useful as these strategies are in many practical applications, they are unlikely to provide submicrometer scale patterns with any significant control over lateral packing and intrinsic defects. In particular, it is now well-appreciated that the monolayer phases within these artificially generated patterns often exhibit nonuniform lateral distributions forming characteristic domains and defect structures, e.g., domain boundaries and pinholes.[8] These often serve as an overlapping and undesirable pattern. On the other hand, it is easily envisaged that these intrinsic domain and defect structures within the film matrix, which result from the thermodynamics and kinetics of monolayer formation,[11] could provide spontaneously generated patterns at much smaller length scales. Further, by control of the monolayer formation process, it appears possible that these domain structures can be tuned to prepare a wide range of self-patterned 2D film architectures. Indeed, Komeda and coworkers[12] have recently reported that *n*-octadecylsiloxane monolayers, derived by retraction from dilute organic solutions, assembled onto oxidized silicon substrates as discrete islands that can serve as self-patterned masks for selective etching of the underlying oxide substrates. By limiting the immersion period, the authors could control the island sizes in a limited range, though a more systematic control over the domain shapes and defect structures using the above approach was evidently difficult to achieve.

Recently, we have been exploring a simple yet highly versatile approach for controlling the structure and defect composition in monomolecular films by directing self-assembly processes using their Langmuir-phase precursors. The equilibrated Langmuir phases, with their rich phase diagrams, provide control of absolute surface coverage, surface phases, and domain characteristics via simple manipulations of subphase parameters, namely temperature, pH, and surface pressure.[13] Transfer of

* Authors to whom correspondence should be sent. E-mail: rwang@lanl.gov, parikh@lanl.gov.

† Bioscience and Biotechnology Group.

10.1021/jp992030y CCC: $18.00
Published on Web 11/03/1999

these preordered Langmuir phases to specific substrate surfaces provides an initial template. This rather weakly held LB film is subsequently stabilized by specific self-assembly events upon recognition of the substrate by the adsorbed monolayer. A recent study by Fang and Knobler[14] has shown the promise of this approach to achieve the control of molecular densities for transferred monolayers of *n*-octadecyltrichlorosilane on acid-treated hydrophilic mica (OTS/mica) substrates by varying the precursor state of the Langmuir monolayers. Their data further reveal pattern formation consisting of small islands (0.4−3.5 μm) when derived from LE phase precursors and the appearance of the coexisting small submicron size domains and larger branched domains (1−1.5 μm) reminiscent of dendritic phases when obtained from LE/LC mixed-phase precursor.

Here we show for a simple, prototypical case of *n*-octadecyltrichlorosilane (OTS) monolayers on oxidized silicon surfaces (OTS/SiO_2/Si) that by carefully selecting appropriate precursor Langmuir phases, the novel lateral packing, domain characteristics, and defect structures in the transferred OTS monolayers at oxidized silicon surfaces can be reproducibly controlled. Our data show a distinct disparity between the pattern structures of the transferred monolayers and their initial equilibrated Langmuir-phase precursors, revealing transfer-induced morphological reconstructions. These reconstructions, driven by surface reorganizations and increased condensation at the substrate surface, can be understood in terms of a balance of competing short range attractive and long-range repulsive interactions. Furthermore, we observed that while the dominant morphological features were independent of the transfer rate, this rate was found to strongly influence the precise domain structures, sizes, and distributions, thereby indicating a nonequilibrium aspect of the final pattern formation. This rate dependence of film morphologies can be understood in terms of the previously proposed model[14] involving the pulling rate dependent variations in the thickness of the intervening water layer. Note that despite considerable similarity in our OTS/SiO_2/Si system and the previously studied OTS/mica system,[14] the morphologies of OTS/SiO_2/Si phases and their correlations with the precursor Langmuir state are dramatically different from those reported for OTS/mica.

Experimental Section

Langmuir Isotherms and LB Depositions. Aliquots of 25−50 μL of 1 mg/mL solution of octadecyltrichlorosilane (Aldrich) in 2:1 V/V chloroform /methanol mixture were spread drop-by-drop on the pure-water subphase surface of a constant perimeter Langmuir trough (NIMA Technologies, Coventary, England). The subphase condition, pH = 5.6 and temperature $T = 20.4 \pm 0.4$ °C, was controlled for all preparations reported here. To ensure complete evaporation of the solvent phase, the subphase surface was left standing for at least 45 min. Compression isotherms were collected in a quasi-static mode with barrier velocities of 10 cm^2/min. Monolayer transfers to solid substrates were carried out at surface pressures of 7.8, 20, and 30 mN/m, each at four different pulling rates of 5, 10, 25, and 43 mm/min. Only single monolayers were transferred during the upstroke withdrawal of substrates from the subphase medium as judged by transfer ratios, which were found to be 100% ± 15% within experimental error. All samples emerged visibly dry and were immediately subjected to further characterization.

Single Wavelength Ellipsometry. A null ellipsometer (Rudolph Research, Piscataway, NJ) operating at 632.8 nm and at a 70° angle of incidence was used with a beam area of ~4 mm^2. Measurements were made at three different spots on each sample. The instrumental precision of the ellipsometric angles was 0.04° and the overall sample-to-sample errors in average calculated OTS film thicknesses are within ±2 Å. OTS film thicknesses were determined using standard electromagnetic treatment for a parallel-layer model consisting of an air/monolayer/substrate structure.[15] The calculations were performed by assuming the isotropic refractive index of $n_i = 1.50$ for densely packed films[16] and $n_i = 1.44$ for low coverage films, composed essentially of conformationally disordered films.[17] Strictly speaking, these approximations are not correct for discontinuous or heterogeneous structures (see below). Using the Maxwell−Garnett effective medium approximation (EMA) for an accurate modeling of the mixed morphology films[18] confirmed that the uncertainties introduced by neglecting the structural heterogenieties of transferred films were ±2 Å, within the experimental error in our measurements.

Atomic Force Microscopy. AFM measurements were performed using a NanoScope III system from Digital Instruments (Santa Barbara, CA) with a 125 × 125 μm scanner. Samples were cut into 1 × 1 cm square pieces, mounted onto standard sample holders. Commercial silicon cantilevers were used to acquire images in tapping mode at a resonant frequency of ~340 kHz under ambient conditions. All the images illustrated in this paper are in height mode, and have been adjusted to the same contrast level for direct comparisons. Images were obtained with 512 × 512 points with scanning rates from 1.0 to 3.0 Hz/line.

Results

A typical compression isotherm obtained for prepolymerized OTS monolayers at the air−water interface under the subphase conditions of pH = 5.6 and $T = 20.4$ °C is shown in Figure 1. Four distinct regions are evident in the isotherm: an initial flat portion (I) at ~0 mN/m at molecular areas > 0.55 nm^2/molecule; a limb of rising surface pressures (II) between molecular areas of ~0.55−0.35 nm^2/molecule and surface pressures of 0−17 mN/m; a distinct plateau-like region (III) between molecular areas of ~0.35−0.25 nm^2/molecule and surface pressures of 19−21 mN/m; and a steep ramp of rapidly rising surface pressures (IV) between ~26−58 mN/m in the lowest molecular area range of ~0.25−0.18 nm^2/molecule. The marked locations (indicated by arrows) along the isotherm in Figure 1 indicate the surface pressures (and corresponding molecular areas) at which the prepolymerized OTS films were transferred onto SiO_2/Si substrates. Ellipsometrically derived film thicknesses of 2.7, 2.1, and 1.6 nm for the transferred films (OTS/SiO_2/Si) obtained from LC, LE/LC, and LE phase precursors suggest the correspondence between the OTS/SiO_2/Si films and the average molecular densities in their corresponding precursor phases. These values are qualitatively consistent with near unity transfer ratios noted during the film preparation. Also shown in Figure 1 are typical AFM images that reveal pronounced differences in the mesoscale surface morphologies, all prepared using the lowest transfer rate of 5 mm/min examined in this study. Concentric ring-shaped and circular-shaped domain features appear in the images of monolayers transferred at 7.8 and 20 mN/m respectively, while the monolayers transferred at 30 mN/m show a uniform surface structure with little evidence for the formation of domain structures.

All the pattern structures obtained in this study showed great thermal and chemical stability. AFM images confirmed that the general characteristics of the patterns did not change upon multiple solvent rinses (e.g., chloroform, acetone, and ethanol), ultrasonication, or mild annealing at up to 100 °C for ~1 h.

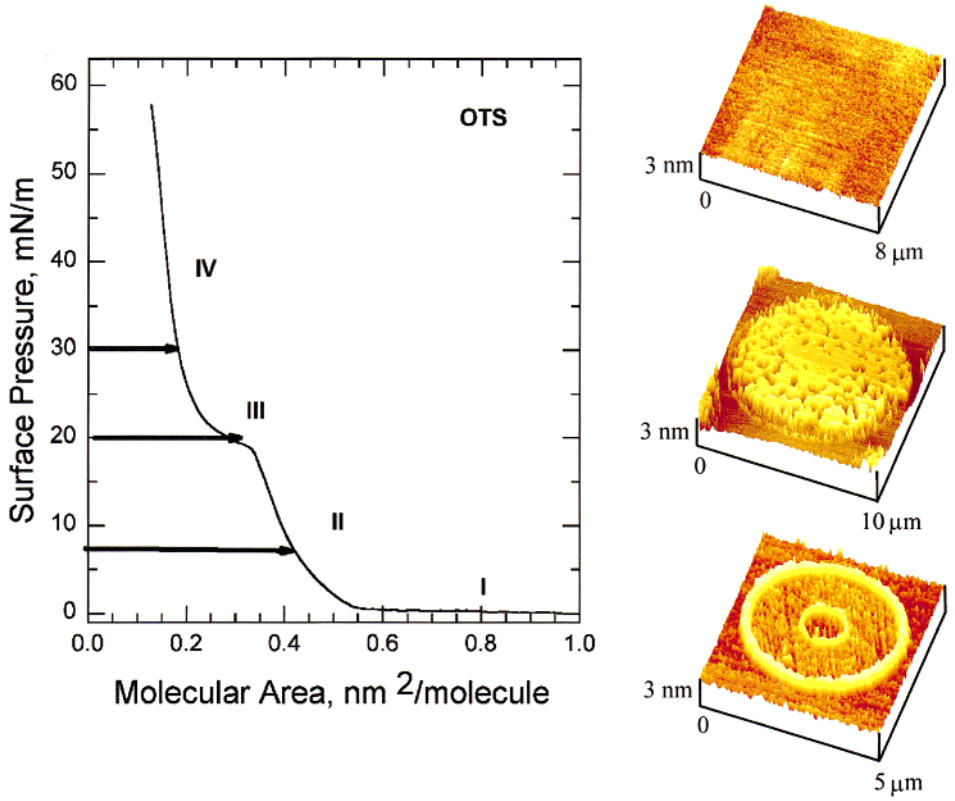

Figure 1. Compression isotherm of the prepolymerized OTS monolayer at the air−water interface, as well as typical AFM images of substrate supported monolayers on SiO_2/Si substrates transferred at 7.8, 20, and 30 mN/m, respectively (see text).

In Figure 2, a closer view of the AFM images of the OTS monolayer transferred at 7.8 mN/m at 5 mm/min is shown. Concentric ring-shaped domains with uniform distribution are observed on the surface. The domain size ranges from 2.5 to 7.0 μm. As shown in the larger scale image (Figure 2a), most domains simply contain two concentric rings; however, each domain is distinct in size and the structural detail. In addition to the regular ring-shaped domains, noncircular closed loops, presumably resulting from the overlap of two or more circular rings, are also occasionally observed. The zoom-in image in Figure 2b shows more details of one of the concentric ring domains. Contrasts in the AFM image provide information related to the film topography or lateral differences in heights within the image. Figure 2c and d demonstrate the 1×1 μm images of the outer and inner rings, respectively. The thickness of the outer ring is ∼270 nm, and that of the inner ring is ∼125 nm. The two rings exhibit an identical height of 2.1 ± 0.2 nm (relative to the dark area) as illustrated in the height cross section at the lower panels of Figure 2c and d. Inside the inner ring or between the two rings, a height of 1.0 ± 0.2 nm is measured, also relative to the dark area. In some of the domains, e.g., the one shown in Figure 2b, tall features inside the internal ring were also observed. These features display the same height as those on the two concentric rings.

A typical AFM image obtained for OTS monolayers transferred at 20 mN/m at 5 mm/min is presented in Figure 3. Unlike the concentric ring-shaped domains seen in Figure 2, round-shaped domains with domain sizes of 3−13 μm in diameter appear on the film surface. A careful comparison of Figure 3a with Figure 2a reveals that in the former the lateral separation between neighboring domains becomes smaller, and the domain size larger. In addition, the interior of the domains contains rifts (Figure 3b); however, the solid areas are flat with a relative height of 1.2 ± 0.2 nm with respect to either the area outside the domains or the rifts (dark areas) inside the domains. The results of an ellipsometry measurement indicate the average film thickness of 2.1 nm, even higher than that of 1.6 nm for the film in Figure 2. The AFM image of OTS monolayers transferred at 30 mN/m and 5 mm/min in Figure 4 illustrates solid uniform OTS film morphology with very few defective areas, consistent with the 2.7 nm film thickness from ellipsometry measurement. The height of the flat area of the image, relative to the defect areas, of 1.2 ± 0.2 nm measured from the AFM profile (Figure 4) indicates that the defective areas must contain OTS molecules, but at significantly reduced molecular densities.

The effect of the pulling rate on the structure of the OTS monolayers formed at a surface pressure of 7.8 mN/m and pulling rates ranging from 5 to 43 mm/min is illustrated in Figure 5 and Figure 2. In comparison with Figure 2 (pulling rate of 5 mm/min), the image in Figure 5a shows decorated ring-shaped domains in the film prepared at a pulling rate of 10 mm/min. Additional circular domain walls have formed and joined the original concentric rings from the outside; meanwhile the internal domain walls appear extremely thin (∼40 nm). These additional "budding" rings are considerably smaller than the original "parent" rings. The zoom-in image shown as an inset of Figure 5a shows that the molecular density inside the budding rings is higher than that inside the large rings. Moreover, as revealed in the inset of Figure 5a, the width of the outer ring (314 ± 5 nm) is almost the sum of the width of the inner ring (145 ± 5 nm) and that of the boundary region between the two rings (167 ± 5 nm), indicative of the local splitting of the domain wall for the films prepared at higher pulling rates. The most remarkable feature in Figure 5b (pulling rate of 25 mm/min) is that the width of the domain walls (450−500 nm) is significantly greater than that in Figure 5a (270−320 nm). Most domains still maintain a ring shape, but fewer

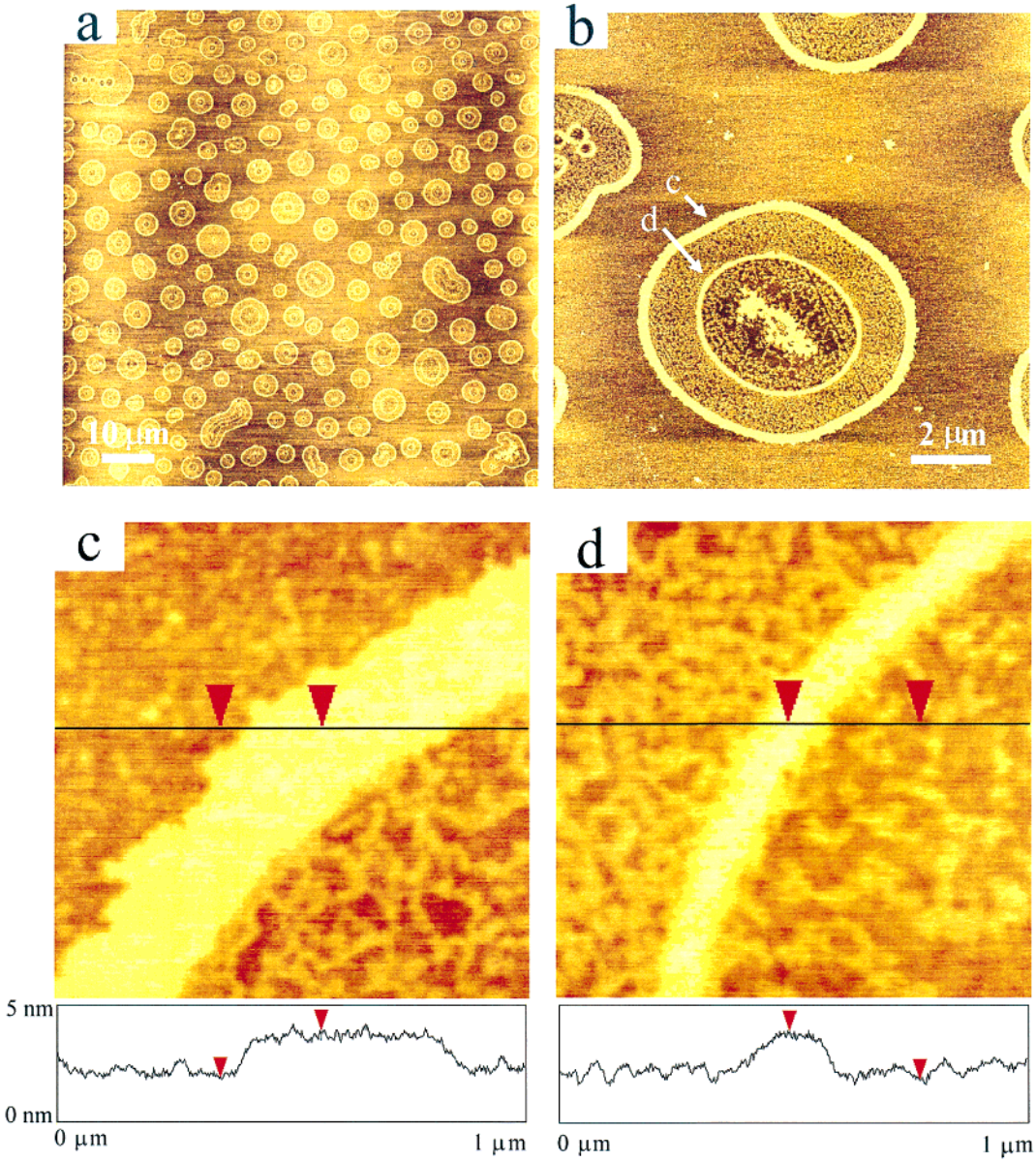

Figure 2. AFM images of OTS monolayer transferred from prepolymerized LE phase Langmuir film (prepared at 7.8 mN/m, pulling rate of 5 mm/min): (a) 90 × 90 μm large scale image; (b) 12 × 12 μm image showing the detailed structures of individual concentric rings; and (c) and (d) zoom-in images (1 × 1 μm) of the outer and inner rings, respectively, as indicated by the arrows in (b). The lower panels illustrate the corresponding height profiles.

domains are decorated with the budding rings. In Figure 5c (pulling rate of 43 mm/min), most domains are distorted from circular shape. Some domains similar to those in Figure 5a can be found, however, with domain walls as wide as 450−500 nm. The others are elongated from circular shape along various directions, showing flowerlike shapes. The ones appearing at the center of Figure 5c are even joined together. In addition, the molecules inside the domain walls are even further decreased in density than in the corresponding regions of the 25 mm/min film (Figure 5b).

Parallel AFM measurements have been performed for monolayers prepared at a surface pressure of 20 mN/m and the same range of pulling rates as above. Images of films at pulling rates of 10, 25, and 43 mm/min respectively are presented in Figure 6, while the image for the pulling rate of 5 mm/min is shown in Figure 3. In comparison with the flat and cracked domain surface seen in Figure 3, the surfaces of the domains in Figure 6a and b appear more uniform and continuous. A closer look at the domain surface (inset of Figure 6a) reveals that the molecular density is slightly lower than for the condensed area inside the domains in Figure 3a. The inset of Figure 6a also illustrates finger structures at the domain boundary, resulting from directional condensation during film transfer.[19] Moving from 10 (Figure 6a) to 25 mm/min (Figure 6b) pulling rates, the domain size becomes larger (7−19 μm in Figure 6a vs 14−22 μm in Figure 6b), and the shape becomes elliptically distorted or irregular polygonal with the increase of pulling rate. In both Figure 6a and b, highly condensed points (bright contrast) appear in approximately the center of the domains, similar to the observation by Wood and Sharma,[20] who ascribed them to the nucleation point of domain growth. When the pulling rate was at the high value of 43 mm/min, most domains appear collapsed, breaking into unstructured patches.

Discussion

Langmuir-Phase Assisted Assembly of Long-Chain Silane Monolayers. Although disagreement continues regarding the

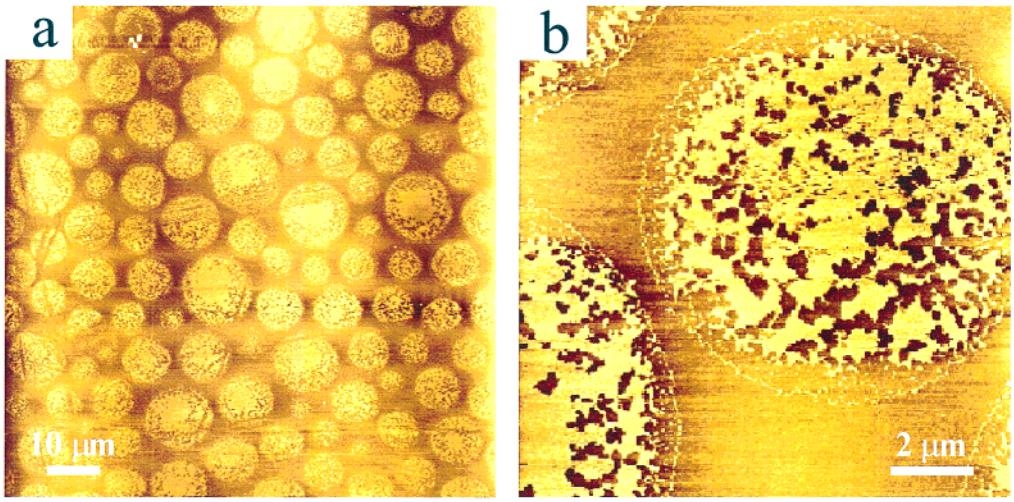

Figure 3. AFM images of OTS monolayer transferred from a prepolymerized LE/LC mixed-phase Langmuir film (prepared at 20 mN/m, pulling rate of 5 mm/min): (a) 90 × 90 μm large scale image and (b) 12 × 12 μm image showing the detailed structure of a typical round-shaped domain.

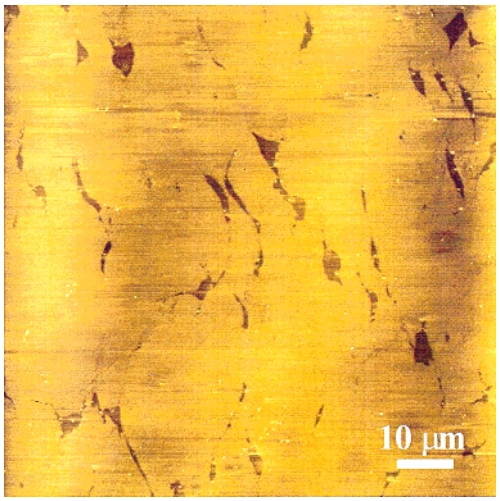

Figure 4. 90 × 90 μm AFM image of OTS monolayer transferred from a prepolymerized LC phase Langmuir film (prepared at 30 mN/m, pulling rate of 5 mm/min).

precise mechanism and kinetics that determine the organic-phase solution self-assembly of OTS monolayers, it is generally well-appreciated that a complex set of surface chemical reactions is involved.[21] At the most simplistic level, these include (1) hydrolysis of the trichlorosilyl headgroup to form trihydroxysilyl derivatives facilitated by the surface bound water; (2) intermolecular condensation of the hydrolyzed species to form an Si−O−Si backbone; and (3) the occasional cross-linking of the oligomer or polymerized species with substrate bound silanol (Si−OH) groups to generate stable monolayer films. In this regard, the results presented in this study have at least one important ramification. The equilibrated precursor Langmuir phase of OTS at the air−water interface requires that the trichlorosilyl headgroup is hydrolyzed and two-dimensionally cross-linked prior to its transfer onto the oxide substrate. The well-behaved amphiphilicity of these preformed species, as evidenced by the pressure−area isotherm (Figure 1) reported here as well as elsewhere,[22] suggests that the first degree ordering of OTS monolayers can occur at the surface of water, even in the absence of the oxide substrate. This evidence is consistent with the notion that the self-assembly of long chain silanes is not primarily determined by substrate−headgroup binding, but by the ability of the surface hydrolyzed and polymerized species to reorganize at the substrate surface to form an organized monolayer phase.[23]

The joint AFM and ellipsometric characterization of the substrate transferred films further highlight the role of substrate chemistry on the Langmuir-phase assisted assembly of OTS monolayers. All the results presented point to the appearance of highly reproducible, characteristic monolayer patterns in the transferred films that depend on the pulling rates and surface pressure. Most of these patterns are unlikely to be present in the corresponding precursor Langmuir phases. The precise nature of the monolayer density, the domain structure, and the defect distributions were found to show unique interrelationships with the surface pressure of the initial Langmuir-phase precursors and the pulling rates. In this manner, the range of patterns obtained is controllable and OTS monolayer films of predetermined surface morphologies can be prepared by appropriately tuning these simple experimental parameters. It is instructive here to compare the pattern structures we observed for OTS/SiO_2/Si with those reported previously for OTS/mica. For the OTS/mica system, Fang and Knobler[14] noted the appearance of a bimodal distribution of small and large islands from LE/LC mixed-phase precursor and uniform islands from LE phase precursor. Our results of formation of very large coalesced domains from LE/LC precursor phase and of the appearance of large ring-in-ring structures from LE phase precursors are in contrast to their observations. We believe this difference arises from the distinct differences in the way the local substrate chemistry (SiO_2/Si vs acid-treated mica) influence the structures of the transferred OTS films. Further, the systematic drive toward increased condensation evident in our data appears not to be the case with OTS/mica wherein the relative distributions of LE and LC phase from the mixed-phase precursor appear to be preserved upon transfer.

Next, our recent preliminary studies suggest that very different types of patterns can also be obtained by variations in subphase conditions including pH, temperature, and ionic strength. A detailed account of these results will be reported separately.[24] Furthermore, the remarkable robustness and stability of these patterns to multiple solvent rinses, mild thermal annealing, and laboratory storage in excess of one month clearly distinguish these monolayers from typical Langmuir−Blodgett films, which dissipate during such treatments. This enhanced stability likely derives from self-assembly events, namely occasional substrate binding, that follow the transfer of the OTS films to SiO_2/Si

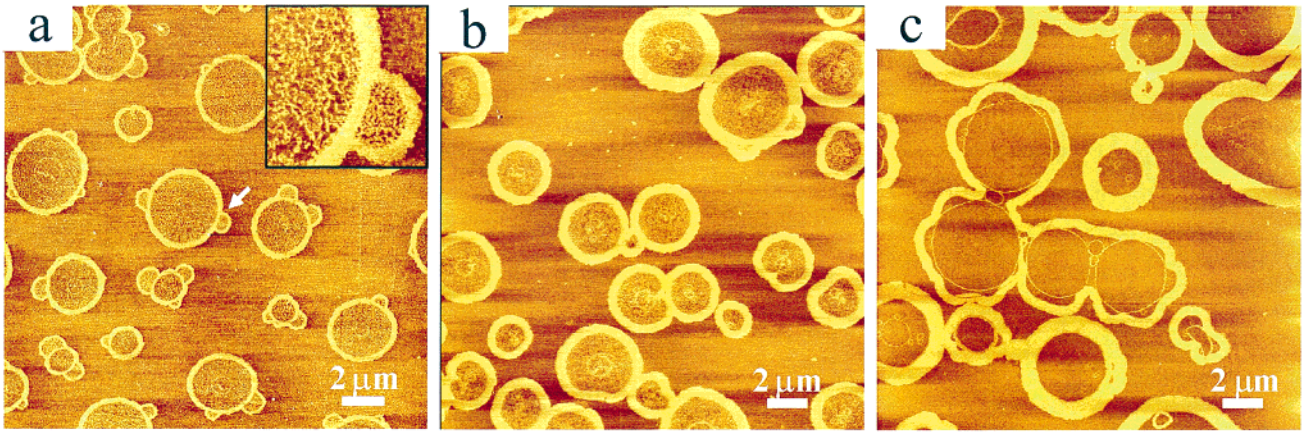

Figure 5. Pulling rate dependence of domain structures for an OTS monolayer transferred at 7.8 mN/m: (a) 10, (b) 25, and (c) 43 mm/min. The image size is 20 × 20 μm. Inset of (a) shows the enlarged image of the arrow-pointed area (1.8 × 1.8 μm). For 5 mm/min, see Figure 2.

substrates. Below, we discuss our observations regarding the detailed structures of the transferred patterns in relation to their Langmuir-phase precursors, and offer plausible mechanisms that may explain the formation of the pattern structures.

Correlations between the Structures of the Transferred OTS Films and their Precursor Langmuir Phases. The phase characteristics of the precursor Langmuir monolayers at the air−water interface can be easily deduced for a given applied pressure from their pressure−area isotherms. For the three deposition pressures of 7.8, 20, and 35 mN/m used in the present study, the precursor OTS monolayers can be straightforwardly assigned to liquid expanded (LE), liquid expanded and liquid condensed (LE/LC) coexistence, and liquid condensed (LC) phases, respectively. These assignments, made in direct analogy with a large body of literature dealing with comparable assignments and structural characterization for typical amphiphiles at the air−water interface,[25] provide a very reasonable structural description of the precursor phases. Based on these assignments, the equilibrated OTS monolayers (at the air−water interface) at 7.8 and 30 mN/m in their LE and LC phases can be described as homogeneous single phases, whereas that at 20 mN/m can be assigned to a mixed LE/LC phase. The LE phase at 7.8 mN/m is a uniform low density phase wherein the molecules at intermediate liquidlike densities experience each other and have partial short range orientational order but little or no long range translational order. The LC phase, by contrast, can be regarded as a two-dimensional solid wherein molecules are packed at limiting densities in an ordered structure and exhibit significant orientational preference and translational ordering. The precursor OTS monolayer at 20 mN/m residing in the LE/LC coexistence phase consists simultaneously of local regions of LE and LC.

By contrast, the substrate transferred monolayers from each of the above precursors are characterized by inhomogeneities, defects, and the presence of two or more regions of distinctly different molecular densities and thereby phase characteristics. The OTS/SiO_2/Si films prepared from the LC precursor phase at 30 mN/m shows a rather uniform surface topology (Figure 4) with isolated defects. The height disparity of 1.2 ± 0.2 nm between the depressions at the defect regions and the film surface in comparison with the estimated LC phase height of 2.62 nm[26] clearly suggests that the defect sites are not vacant, but must also be occupied with OTS molecules. Based on the above, we estimate that the molecular density of OTS molecules in the depression is approximately 55% (=(2.62 − 1.2)/2.62 × 100%) of the LC phase. By taking the surface density of 0.2 nm^2/molecule for the LC phase estimated from the Π-A isotherm in Figure 1, we infer that the molecular density of OTS corresponds to approximately 0.36 nm^2/molecule. This value suggests that OTS molecules in the defect regions are at a molecular density comparable to a typical LE phase. Thus, we conclude that the transferred OTS films obtained from the LC phase Langmuir precursor are also dominantly in the LC phase, but possess uniformly distributed defects (below 10% average population) of regions corresponding to the LE phase. This general morphology for OTS films prepared from the LC phase precursor is independent of the rate of transfer.

When the precursor OTS Langmuir film is in the pure LE phase at 7.8 mN/m, the transferred films show a large number of two concentric ring units uniformly distributed across the substrate surface. The sizes of these circular units depend on the pulling rate; and the distribution of the rings does not show any long range translational ordering. Each ring structure is composed of two concentric rings whose walls are 2.1 (± 0.2) nm higher than the outer background, but only 1.1 (± 0.2) nm higher than the encircled region. The ring walls can be clearly attributed to a solid LC-like phase. The entrapped region, by an analysis similar to the above, is composed of a lower density LE-like phase at ∼0.35 nm^2/molecule and the outer background contains OTS molecules at about 1.01 nm^2/molecule, analogous to the G phase.

The OTS/SiO_2/Si films produced by transferring the LE/LC mixed-phase precursor Langmuir monolayer also reveal a peculiar pattern structure consisting of closely packed circular, elliptical, or polygonal domains. The shapes and sizes are variable and depend strongly on the pulling rate. The height of the polygonal domains with respect to the interdomain background is 1.2 nm, which reveals the coexistence (see above), of LC-like phase (domains) with regions in the grain-boundary at the molecular densities comparable to LE phase.

Taken together, the phase assignments above reveal two important features of the Langmuir-phase assisted assembly of OTS monolayers. Note that in all the substrate transferred films, regardless of the phase state of the precursor OTS Langmuir monolayer, the LC-like phase is present. This alone provides a compelling indication that one effect of the substrate on the OTS monolayers is to induce a local condensation transition. Similar condensation transitions in conventional Langmuir−Blodgett films have been recently reported.[27] In that study, Schwartz and co-workers show that LB films of penta- and hexadecanoic acids at a mica surface prepared by transferring their precursor LE Langmuir phases showed densely packed islands similar to those obtained when the precursor Langmuir monolayer is in the LC phase. They further postulate that this

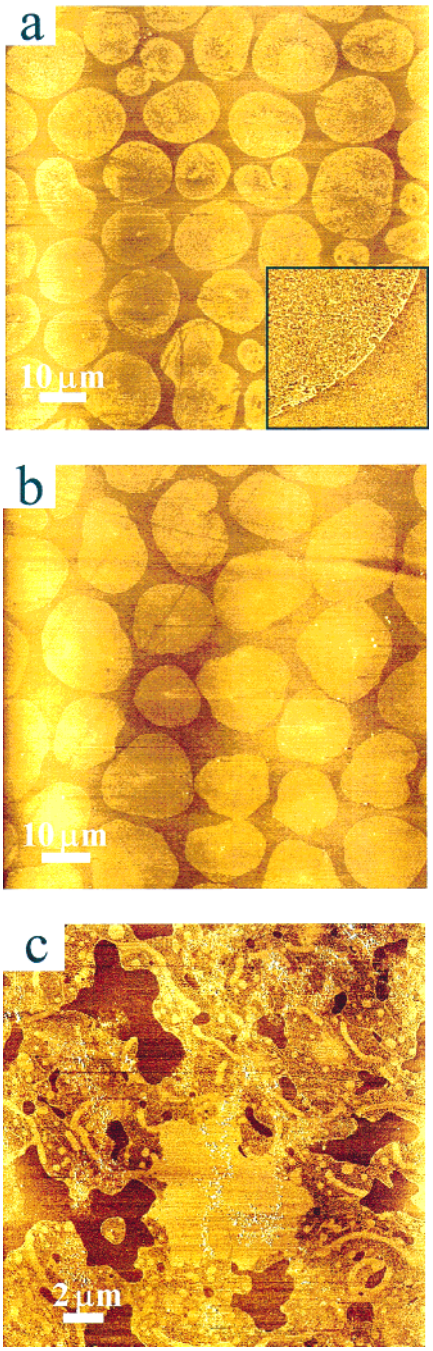

Figure 6. Pulling rate dependence of domain structures for an OTS monolayer transferred at 20 mN/m: (a) 10, (b) 25, and (c) 43 mm/min. The image size is 90 × 90 μm for (a) and (b), and 20 × 20 μm for (c). Inset of (a) illustrates the domain boundary, with image size of 5 × 5 μm. For 5 mm/min, see Figure 3.

condensation process might be due to the surface tension gradient[28] experienced by the growing monolayer during the film transfer.

The Pulling Rate Dependence. One of the key factors that influence domain structures is the pulling rate. This dependence requires that the pulling rate must influence monolayer nucleation and growth during film transfer.

It has been previously suggested that the higher pulling rate reduces the time available for drainage of the prewetting water layer from the substrate surface.[14] Thus, when the substrate is pulled from the Langmuir trough rapidly, a thicker water layer must remain at the substrate surface. It is quite reasonable to assume that such an intervening water layer masks the substrate chemistry and enhances molecular diffusion and mobility, thereby promoting more efficient self-organization of OTS molecules at the substrate surface. The series of AFM images in Figure 5 is consistent with such a description. At the pulling rate of 10 mm/min, most domain walls of the rings are locally split, forming one or more small budding rings decorating the original parent rings. This can be rationalized to result from the disturbance of the initial domain structure due to enhanced surface reorganization at a higher pulling rate. At even higher pulling rates, we observe an increase in the width of the domain walls and a concomitant decrease in the molecular density of the LE phase it entraps (Figures 2a and 5). This observation is also consistent with the more efficient surface reorganization with increased pulling rate, leading to LC phase formation at the expense of disordered LE phase. Another important attribute of the images for the films produced at higher pulling rates (25 mm/min and 43 mm/min) is the observed coalescence of neighboring domains (Figure 5). This process, occurring concurrently with the lowering of the LE phase population or condensation transition, can be ascribed to a very different type of transient surface diffusion of the individual LC phase domains at the substrate surface during film formation.

The pulling rate also changes the characteristics of the round shaped domains formed from LE/LC precursors in Figure 6. With the increased pulling rate, domain sizes appear larger, less circular, and the lateral separation between neighboring domains is smaller. It has been previously assumed that when the water layer dries on the substrate surface, the LE phase molecules at the interdomain regions are compressed into the LC phase and contribute to the growth of the LC domains.[14] This assumption is consistent with our observation of the reduced domain separation at higher pulling rates, which in turn is indicative of the decrease of the amount of OTS molecules in the LE phase and the increase in the LC phase.

The uniform, solid films formed from LC phase precursors are scarcely influenced by the pulling rate. This insensitivity is attributed to the low diffusion and mobility of the individual molecules in the continuous solid films even at the air−water interface. Hence the films are only slightly affected by the transfer process.

We further note that the rifts observed at low pulling rates (Figure 3) are replaced, at the higher pulling rates (10 and 25 mm/min), by more uniform, but lower surface density, domain tops. We believe this must occur by a slight relaxation of the molecules within each domain. This can also be attributed to the thicker water layer transferred onto the substrate surface at high pulling rates, which favors molecular diffusion.

It is interesting to note that at the highest (43 mm/min) pulling rate examined in this study, the domain structure is completely replaced by a collapsed amorphous film structure (Figure 6c) and the film thickness measured by ellipsometry exceeds monolayer coverage. This may be due to high water content at the substrate surface coupled with a larger number of OTS molecules for films prepared at LE/LC (in comparison with the LE phase film), leading to uncontrollable additional cross-linking of silyl headgroups to form 3D clusters.

Plausible Mechanisms for the Pattern Formation. All the data presented here can be reconciled in a simple phenomenological description for the pattern formation. The description is based on the restricted surface reorganization of the transferred monolayer phase. Two major restrictions include (1) starting Langmuir-phase monolayer density which limits the range of patterns observed; and (2) the drainage of the substrate-bound interfacial water and/or occasional substrate pinning of the

monolayer phase, which arrrests the pattern evolution. Before we proceed to explore its implications, we first recapitulate the essential features of this description brought out by the results presented here. First, it is evident that, across the series of sample systems investigated here, there is a clear drive toward increased condensation (see above). This observation requires reconstruction of the initial Langmuir phase during or upon the transfer to oxide substrates. The monolayer reorganization is also directed toward the formation of the condensed phase since the reorganization invariably results in the local appearance of the LC phase in the monolayer patterns. Second, the fact that the surface density of the transferred OTS monolayers show a direct correlation with that of the starting precursor phase at the air−water interface (as judged from the near unity transfer ratios, ellipsometric trends, and AFM images) provides a compelling reason to believe that the monolayer reconstruction occurs only after the initial transfer of the precursor phase is completed. In contrast, a dynamic reconstruction *during the transfer* would most likely result in a disparity between the surface density of the transferred vs precursor monolayer phase,[29] which was not supported by our data. An important implication of this result is that the observed range of patterns are limited by the available number of molecules at the oxide substrate, which in turn is determined by the starting Langmuir-phase precursors. Manifestations of this restriction are amply evident in the very different types of patterns (ring-in-a-ring vs tiled domains) observed depending on the precursor phase density. Third, the observed correlation between the pulling rate and the extent of condensation (see above), as well as the chemical and thermal stability of the monolayer patterns (see results), provide compelling evidence that occasional substrate pinning[30] or drainage of the substrate-bound water[14] must arrest the evolution of the observed patterns. These two processes provide the second restriction in the ranges of patterns observed. Note that the foregoing discussion requiring structural evolution at the substrate surface and dynamic reconstructions establishes the essentially nonequilibrium nature of these patterns. This inference is further supported by noting that in all the transferred films, regardless of the properties of the precursor phase, the simultaneous presence of regions of widely differing molecular densities are evident. This observation cannot be easily reconciled in terms of the equilibrium thermodynamics of 2D interfacial monolayers of single components.[13] Gibbs phase rule ($f = C - P + 2$; where C (number of components) $= 1$: if P (number of distinguishable phases) $= 3$, then f, degrees of freedom, reduces to zero) requires that, for monocomponent 2D monolayers, the coexistence of more than two phases can occur only under a single set of conditions analogous to the 3D triple point substantiating that the transferred monolayers no longer represent the equilibrium thermodynamic character of their Langmuirian precursors. We note that the nonuniformity of the cross-linked OTS oligomers and the possible binding of OTS to the silanols at the substrate surface could render the surface phases to be effectively "multicomponent", and thereby offer a plausible explanation for the emergence of coexisting three phases at the substrate surface. However, even in this scenario, the observed pulling rate dependence strongly indicates that the pattern formation is associated with nonequilibrium effects.

Owing to both the complexity of the structures and the prevailing uncertainties in the current understanding of the silanization process,[23] it is difficult to further develop the phenomenological description above to advance a comprehensive mechanism that captures the details of the pattern structures seen. However, it is possible to gain some insight by drawing analogies with previously reported models of pattern formation in related systems of molecular organic/polymeric films.[31,32]

One of the most widely cited mechanisms for the formation of pattern structures or spatial inhomogenieties in molecular systems (typically binary systems) is based on the competition of short range attractive and long range repulsive interactions.[31] The former favors macroscopic segregation of coexisting phases or components, while the latter tends to minimize domains of single phases or components in mixed-phase or multicomponent systems. In a continuum description of monolayer phases[33] such as here, the average long range repulsive force can be understood to arise from the pairwise interactions between the headgroup dipole moment vectors (which are nominally aligned perpendicular to the film surface). This repulsive interaction competes with the short range line tension which represents the energy cost associated with the local variations in molecular density or concentration.

Our observations of the formation of ring-in-a-ring structures (Figure 2) from the LE phase precursor and the formation of circular domains (Figure 3) from the LE/LC phase precursor can be qualitatively understood in terms of these models of competing interactions. The circular shape of the LC phase domains appear to reflect the local dominance of the line tension term,[33] whereas the finite sizes of the LC phase domains (in contrast to a single large LC phase domain) suggest the overall optimal balance determined by the contribution from the competing dipole−dipole repulsive energy. This inference is further substantiated by the observation that, in both the ring-in-a-ring and the tiled domain morphologies, the LC phase domain sizes are systematically larger (Figures 5 and 6) at higher pulling rates (or greater condensation). This observation appears qualitatively consistent with the competing interaction model since the changes in the relative populations of the LC and LE phases, caused by variations in the pulling rate, must alter the balance of the competing interactions to favor the dominance by the line tension term over dipolar repulsion.

Conclusions

Results presented here for the OTS/SiO2/Si system and related results for OTS/mica reported previously by Fang and Knobler suggest that the Langmuir-phase assisted assembly of prepolymerized long chain silane monolayers onto oxide substrates offers a useful alternative to the solution-phase self-assembly approach. The OTS films prepared by this approach show remarkably stable surface monolayers in sharp contrast to the conventional Langmuir−Blodgett films. The surface density of the transferred monolayers can be controlled to predetermined submonolayer values by simply varying the surface pressure, and hence the initial phase, of the precursor Langmuir film. Moreover, precise lateral distribution or types of pattern structures in the transferred films can also be controlled by simple variations in the pulling rate. For example, the OTS monolayers formed from the LE phase precursor exhibit unique ring-in-a-ring morphology not observed previously for any Langmuir−Blodgett films wherein two concentric walls of LC phase OTS molecules sandwich and encapsulate disordered OTS molecules in the LE phase. On the other hand, the monolayers formed from the LC/LE phase precursor reveal uniform tiling of near-circular domains composed of ordered OTS molecules in the LC phase. The monolayers derived from the 2D solid or LC precursor state reveal near-complete surface coverages and uniform film structures. These patterns appear to form by restricted structural reconstructions at the substrate surface causing condensation transitions. The observed pattern

formation and pulling rate dependences are qualitatively rationalized in terms of competing short range attractive (line tension) and long range dipolar repulsive interactions.

Acknowledgment. R.W. acknowledges the support of a Director's Fellowship at Los Alamos National Laboratory. This work was supported by the LDRD program at Los Alamos National Laboratory.

References and Notes

(1) Singhvi, R.; Kumar, A.; Lopez, G. P.; Stephanopoulos, G. N.; Wang, D.; Whitesides, G. M.; Ingber, D. E. *Science* **1994**, *264*, 696.

(2) Gau, H.; Herminghaus, S.; Lenz, P.; Lipowsky, R. *Science* **1999**, *283*, 46.

(3) Wang, R.; Hashimoto, K.; Fujishima, A.; Chikuni, M.; Kojima, E.; Kitamura, A.; Shimohogoshi, M.; Watanabe, T. *Nature* **1997**, *388*, 431.

(4) Gibbons, W. M.; Shannon, P. J.; Sun, S. T.; Swetlin, B. J. *Nature* **1991**, *351*, 49.

(5) Hickman, J. J.; Laibinis, P. E.; Auerbach, D. I.; Zou, C. F.; Gardner, T. J.; Whitesides, G. M.; Wrighton, M. S. *Langmuir* **1992**, *8*, 357.

(6) (a) Behm, J. M.; Lykke, K. R.; Pellin, M. J.; Hemminger, J. C. *Langmuir* **1996**, *12*, 2121. (b) Lercel, M. J.; Redinbo, G. F.; Pardo, F. D.; Rooks, M.; Tiberio, R. C.; Simpson, P.; Craighead, H. G.; Sheen, C. W.; Parikh, A. N.; Allara, D. L. *J. Vac. Sci. Technol. B* **1994**, *12*, 3663.

(7) Lopez, G. P.; Biebuyck, H. A.; Frisbie, C. D.; Whitesides, G. M. *Science* **1993**, *260*, 647.

(8) Jeon, N. L.; Finnie, K.; Branshaw, K.; Nuzzo, R. G. *Langmuir* **1997**, *13*, 3382.

(9) Nuzzo, R. G.; Allara, D. L. *J. Am. Chem. Soc.* **1983**, *105*, 4481.

(10) (a) Sagiv, J. *J. Am. Chem. Soc.* **1980**, *102*, 92. (b) Netzer, L.; Sagiv, J. *J. Am. Chem. Soc.* **1983**, *105*, 674.

(11) Bierbaum, K.; Grunze, M.; Baski, A. A.; Chi, L. F.; Schrepp, W.; Fuchs, H. *Langmuir* **1995**, *11*, 2143.

(12) Komeda, T.; Namba, K.; Nishioka, Y. *Appl. Phys. Lett*. **1997**, *70*, 3398.

(13) Gaines, G. L., Jr. *Insoluble Monolayers at Liquid−Gas Interfaces;* Wiley-Interscience: New York, 1966 and selected references therein.

(14) Fang, J. Y.; Knobler, C. M. *J. Phys. Chem.* **1995**, *99* (*26*), 10425. Fang, J. Y.; Knobler, C. M. *Langmuir* **1996**, *12*, 1368.

(15) Azzam, R. M. A.; Bashara, N. M. *Ellipsometry and Polarized Light;* North-Holland: Amsterdam, The Netherlands, 1977.

(16) *Polymer Handbook*; Brandrup, J., Immergut, E. H., Eds.; John Wiley: New York, 1975; Vol. 13. p. V-22.

(17) Thoma, M.; Schwendler, M.; Baltes, H.; Helm, C. A.; Pfohl, T.; Riegler, H.; Mohwald, H. *Langmuir* **1996**, *12*, 1722.

(18) See, for example: Frey, W.; Schief, W. R.; Vogel, V. *Langmuir* **1996,** *12*, 1312.

(19) Chi, L. F.; Fuchs, H.; Johnston, R. R.; Ringsdorf, H. *Thin Solid Films* **1994**, *242*, 151.

(20) Wood, J.; Sharma, R. *Langmuir* **1995**, *11*, 4797.

(21) Ulman, A. *Chem. Rev.* **1996**, *96*, 1533.

(22) Barton, S. W.; Goudot, A.; Rondelez, F. *Langmuir* **1991**, *7*, 1029.

(23) Parikh, A. N.; Allara, D. L.; Azouz, I. B.; Rondelez, F. *J. Phys. Chem.* **1994**, *98*, 7577.

(24) Wang, R.; Parikh, A. N.; Beers J. D.; Shreve A. P.; Swanson, B. I., manuscript in preparation, 1999.

(25) See, for example: Knobler, C. M. *Science* **1990**, *249*, 870.

(26) Wasserman, S. R.; Whitesides, G. M.; Tidswell, I. M.; Ocko, B. M.; Pershan, P. S.; Axe, J. D. *J. Am. Chem. Soc.* **1989**, *111*, 5852.

(27) Sikes, H. D.; Schwartz, D. K. *Langmuir* **1997**, *13*, 4704.

(28) Spratte, K.; Chi, L. F.; Riegler, H. *Europhys. Lett.* **1994**, *25*, 211.

(29) Sikes, H. D.; Woodward, J. T.; Schwartz, D. K. *J. Phys. Chem.* **1996**, *100*, 9093.

(30) (a) Tripp, C. P.; Veregin, R. P. N.; Mcdougall, M. N. V.; Osmond, D. *Langmuir* **1995**, *11*, 1858. (b) Tripp, C. P.; Hair, M. L. *Langmuir* **1995**, *11*, 1215.

(31) See, for example: (a) Seul, M.; Andelman, D. *Science* **1995**, *267*, 476. (b) Seul, M.; Sammon, M. J. *Phys. Rev. Lett.* **1990**, *64*, 1903.

(32) (a) Reiter, G. *Phys. Rev. Lett.* **1992**, *68*, 75. (b) Reiter, G. *Science* **1998**, *283*, 888.

(33) (a) McConnell, H. M.; Moy, V. T. *J. Phys. Chem.* **1988**, *92*, 4520. (b) Andelman, D.; Brochard, F.; Joanny, J. F. *J. Chem. Phys.* **1987,** *86*, 3673.